JOURNAL OF AGRICULTURAL AND FOOD CHEMISTRY

Article

Cite This: J. Agric. Food Chem. 2019, 67, 11331−11339

pubs.acs.org/JAFC

Systematic Evaluation of Chiral Fungicide Imazalil and Its Major Metabolite R14821 (Imazalil-M): Stability of Enantiomers, Enantioselective Bioactivity, Aquatic Toxicity, and Dissipation in Greenhouse Vegetables and Soil

Runan Li,[†] Xinglu Pan,[†] Yan Tao,[†] Duoduo Jiang,[†] Zenglong Chen,[‡] Fengshou Dong,*[,†] Jun Xu,[†] Xingang Liu,[†] Xiaohu Wu,[†] and Yongquan Zheng[†]

[†]State Key Laboratory for Biology of Plant Diseases and Insect Pests, Institute of Plant Protection, Chinese Academy of Agricultural Sciences, Beijing 100193, P. R. China

[‡]State Key Laboratory of Integrated Management of Pest Insects and Rodents, Institute of Zoology, Chinese Academy of Sciences, Beijing 100101, P. R. China

Supporting Information

ABSTRACT: Chiral pesticides are often produced and applied without distinguishing the difference of enantiomers, which sometimes leads to overuse and inaccurate risk assessment. Imazalil is a widely used chiral fungicide; its parent and major metabolite R14821 (imazalil-M) are usually detected in environmental and plant samples. The enantioselective bioactivity of imazalil enantiomers to seven typical pathogens (e.g., *Fulvia fulva*) was explored. *S*-(+)-Imazalil showed 3.00−6.59 times higher bioactivity than its antipode for selected pathogens. Molecular docking partly explained the mechanism of enantioselectivity in bioactivity. *S*-(+)-Imazalil had a stronger hydrophobic interaction and lower energy conformation with binding sites than *R*-(−)-imazalil. The acute toxicity of *S*-(+)-imazalil was 1.23-fold and 2.25-fold more than *R*-(−)-imazalil to *P. subcapitata* and *D. magna*, respectively. And, *S*-(+)-imazalil-M had 2.21-fold and 1.70-fold higher toxicity than *R*-(−)-imazalil-M to *P. subcapitata* and *D. magna*, respectively. However, *R*-(−)-imazalil was 1.21 times more toxic than *S*-(+)-imazalil to *D. rerio*. The enantioselective dissipation of imazalil and imazalil-M was explored under greenhouse conditions. High-effective *S*-(+)-imazalil preferentially enriched in leaf and fruit of tomato and cucumber, and no enantioselective degradation was found in soil. Imazalil-M enantiomers formed in cucumber, leaf of cucumber, and tomato, and the EF values fluctuated between 0.332 and 0.499. The results could provide information for more accurate assessment of imazalil; they implicated that using *S*-(+)-imazalil could reduce pesticide input and the risk to *D. rerio*.

KEYWORDS: *imazalil, metabolite, enantioselective bioactivity, aquatic toxicity, dissipation*

INTRODUCTION

Pesticides are important in reducing the yield loss of crops; meanwhile, they need to be assessed and controlled to ensure food safety and environmental health considering their potential risk.[1] Although chiral pesticides are estimated to account for approximately 30% to 40% of registered pesticides in the world market, the majority of them are sold as racemate.[2,3] Stereoisomers of chiral pesticides often show enantioselectivity in bioactivity; therefore, many single isomer products have continued to be registered to reduce the usage of pesticides.[3,4] Many highly effective chiral monomers have lower toxicity to nontarget organisms, which would be beneficial for the environment.[5,6] Thus, it is important to explore the difference between enantiomers of chiral pesticides to offer recommendations on developing the products of single enantiomers. Furthermore, pesticides may transform to potentially hazardous metabolites in the environment. For instance, triadimefon is less toxic than its metabolite triadimenol to many nontarget organisms.[7] Thus, systematic evaluation of the enantioselectivity of chiral pesticides and the toxicological effects of their metabolites of pesticides is essential for accurate risk assessment and rational application of chiral pesticides.

Imazalil (Figure 1) is a widely used chiral fungicide which is applied in the cultivation of fruit and vegetables, including cucumber and tomato, in postharvest treatment and which is also used as an antimycotic drug.[8] The major metabolite of imazalil (R14821), 1-(2, 4-dichlorophenyl)-2-(1H-imidazole-1-yl)-1-ethanol (imazalil-M), also possesses a chiral center (Figure 1). Imazalil-M is a synthetic intermediate of imazalil. The relatively stable imazalil-M was often detected in many agricultural products (grapefruit, orange, lemon), and wetland plants in plant uptake studies.[9−12] However, these studies are limited to racemate. Imazalil is sold and applied as racemate even today. In 2001, a patent reported that *S*-(+)-imazalil has stronger bioactivity than its antipode tested on target fungi including *Phytophthora infestans* (occurred in tomato), *Pyricularia oryzae* (occurred in rice), *Botrytis cineria* (occurred

Received: June 20, 2019
Revised: September 9, 2019
Accepted: September 17, 2019
Published: September 17, 2019

Downloaded via UNIV OF ALABAMA BIRMINGHAM on October 21, 2019 at 16:12:11 (UTC).
See https://pubs.acs.org/sharingguidelines for options on how to legitimately share published articles.

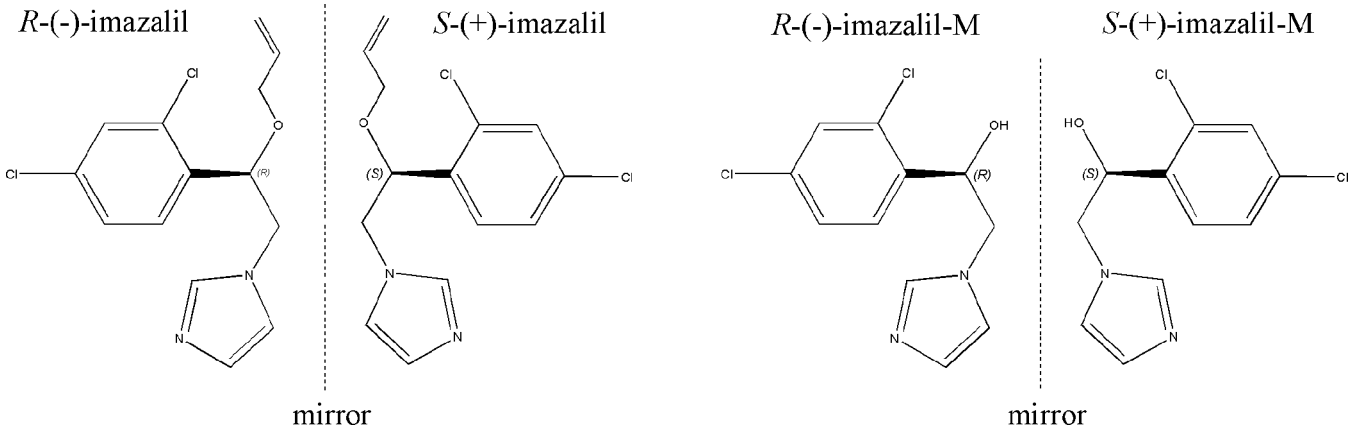

Figure 1. Chemical structure of enantiomers of imazalil and its major metabolite R14821 (imazalil-M).

in pepper), *Erysiphe graminis* (occurred in wheat), and *Puccinia recondite* (occurred in wheat).[13] However, the difference of bioactivity between imazalil enantiomers on other fungi like *Fulvia fulva, Alternaria solani, Glomerella cingulate, Valsa mali,* and *Penicillium digitatum* has not been investigated, which directly hinders the development of the high-effective enantiomer of imazalil. Furthermore, the mechanism of enantioselective bioactivity has not been revealed.

Due to the extensive application of imazalil in agricultural products and postharvest treatment of fruits, imazalil may enter water in the environment and pose an ecological threat to aquatic organisms. It has been frequently detected in water samples in recent years; imazalil reached a maximum concentration level of 409.76 ng/L in Ebro River in Spain for two years and showed risk toward daphnia and fish at mean and maximum concentrations.[14] The highest concentration of imazalil was 172 ng/L in the Júcar River in the 2010 and 750 ng/L in the Turia River between 2012 and 2013.[15,16] The composition of macroinvertebrate communities would be damaged even when the concentration of imazalil exceeded 1 μg/L in aquatic environments.[17] It also has potential developmental toxicity and neurobehavioral toxicity in zebrafish.[18] However, the toxicity assessment of imazalil is based on the racemate without distinguishing the potential toxicity difference between the two enantiomers, which may lead to inaccuracy in risk assessment and difficulties in recommending an enantiomer-pure product of imazalil. Moreover, the toxicity study of the metabolite of imazalil is limited especially at enantiomeric level. These would pose an unknown risk of imazalil to human health and environmental safety.

The enantioselective dissipation of imazalil has been reported in oranges, wetland plants, and apples.[12,14,19−21] Enantioselective trends differed according to species, varieties, and different parts of plants. Therefore, we investigated the enantioselective dissipation of imazalil and its metabolite in tomato, cucumber, and soil under greenhouse conditions, and simultaneous enantioseparation of four enantiomers of imazalil and its major metabolite imazalil-M was first reported. The enantioselectivity in bioactivity was measured on seven kinds of pathogens (*Fulvia fulva, Alternaria solani, Phytophthora infestans, Botrytis cinereal, Glomerella cingulate, Valsa mali,* and *Penicillium digitatum*). The acute toxicity of enantiomers of imazalil and imazalil-M toward several aquatic organisms (*P. subcapitata*, *D. magna*, and *D. rerio*) was explored. Comprehensive assessments of enantioselective bioactivity of imazalil enantiomers, aquatic toxicity, and dissipation in tomato, cucumber, and soil of the four enantiomers were conducted. The results could provide reference for a more accurate risk assessment of imazalil and developing the enantiomer-pure product of imazalil.

MATERIALS AND METHODS

Chemicals and Reagents. Racemic imazalil (purity = 99.2%, enantiomer ratio = 1:1) and its metabolite R14821 (imazalil-M), 1-[2-(2,4-dichlorophenyl)-2-(1*H*-imidazole-1-yl)-1-ethanol] standard (purity = 99.5%, enantiomer ratio = 1:1), were purchased from China Standard Material Center (Beijing, China). Imazalil enantiomers (chemical purity > 99%) were prepared using an HPLC instrument equipped with Superchiral S-OZ column (250 mm length × 21 mm I.D., 5 μm particle size) at 35 °C; the mobile phase was hexane/IPA/DEA (70:30:0.05, v/v/v) pumped at a flow rate of 10 mL/min. Imazalil-M enantiomers (chemical purity > 99%) were prepared using HPLC with a Superchiral S-AD column (250 mm length × 21 mm I.D., 5 μm particle size) at 40 °C; the mobile phase was MeOH/formic acid (100:0.02, v/v), and the flow rate was 10 mL/min. The enantiomeric purity (e.e.%) of the two enantiomers of imazalil and its metabolite exceeded 95% and 98%, respectively. Chromatographic-grade methanol (MeOH) and acetonitrile (ACN) were obtained from Merck KGaA (Darmstadt, Germany). HPLC-grade 2-propanol (IPA) was bought from Thermo Fisher Scientific (Waltham, MA, USA). Analytical pure ammonium formate and ethyl acetate were purchased from Sinopharm Chemical Reagent Co., Ltd. (Shanghai, China). Analytical pure sodium chloride (NaCl), anhydrous magnesium sulfate ($MgSO_4$), and ACN were supplied from Beihua Fine-Chemicals (Beijing, China). Analytical grade acetone and dimethyl sulfoxide (DMSO) were acquired from Beijing Chemical Reagent Co., Ltd. (Beijing, China). Ultrapure water was obtained from the Milli-Q system (Bedford, MA, USA). Primary secondary amine (PSA, 40−60 μm) and graphitized carbon black (GCB, 120−400 mesh) were purchased from Bonna-Agela Technologies (Tianjin, China).

Bioassay of Fungicidal Activity. The bioactivity of imazalil and its two enantiomers were investigated toward seven target pathogens (*Fulvia fulva, Alternaria solani, Phytophthora infestans, Botrytis cinerea, Glomerella cingulate, Valsa mali,* and *Penicillium digitatum*) which were supplied by the Laboratory of Pesticide Bioassay, Institute of Plant Protection, Chinese Academy of Science (Beijing, China). The potato dextrose agar (PDA) medium was prepared from 200 g of potato, 20 g of dextrose, and 20 g of agar for 1 L of distilled water. Different volumes of stock solutions (10000 mg/L in DMSO) of *rac*-imazalil and its enantiomers were added in the test medium which were cooled to 45−50 °C after autoclaving at 120 °C. The concentration of DMSO was no more than 0.1 mg/L. The medium without pesticide was treated as the control. The mycelial plugs (diameter of 5 mm) acquired from the margins of the actively growing colonies were placed in the center of the test PDA plates with different concentrations of target pesticides. Then, the plates were incubated

DOI: 10.1021/acs.jafc.9b03848
J. Agric. Food Chem. 2019, 67, 11331−11339

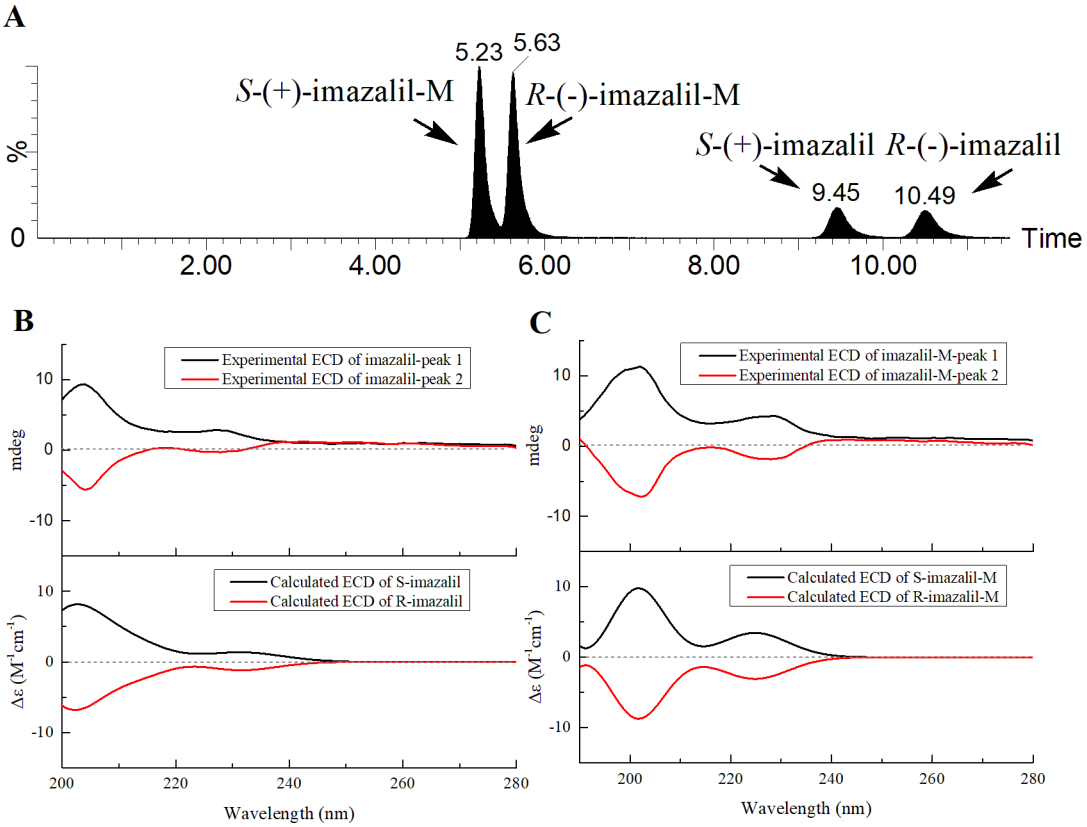

Figure 2. Chromatogram (A) shows the experimentally measured ECD spectrum and computationally calculated ECD spectrum of enantiomers of imazalil (B) and imazalil-M (C).

at 25 °C in the dark (each treatment with three replicates). The colony diameters of all the test PDA plates were measured once the colony diameter of the control reached nearly 7 cm[6].

Toxicity Tests toward Aquatic Organisms. The toxicity tests were conducted in accordance with the Test Guidelines on Environmental Safety Assessment for Chemical Pesticides (GB/T 31270-2014). The green algae (*P. subcapitata*) and *Daphnia magna* organisms were acquired from the Laboratory of Environmental Toxicity, Institute of Plant Protection, Chinese Academy of Agricultural Science (Beijing, China). The green algae were incubated at 23 ± 1 °C with light intensity of approximately 4440 lx in the incubator during the experiment. The zebrafish juveniles (*Danio rerio*) were obtained from local fish supplier (Gaofeng Aquarium Supermarket, Beijing, China) and were raised under laboratory conditions for 2 weeks, and the total length of zebrafish was 2.0 ± 1.0 cm. The water temperature and pH value of water were 26 ± 1 °C and 7.5 ± 0.5 during the test, respectively.

Algal Growth Inhibition Test. The algal cells (at a biomass concentration of about 50000 cells/mL) were grown in an Erlenmeyer flask (250 mL) containing 100 mL of BG11 medium with different treatment concentrations of racemates and enantiomers of imazalil and imazalil-M (stock solutions were prepared in acetone). Each test group and control group (blank control and solvent control) included three replicates with the content of acetone not exceeding 0.1 mL/L. The biomass concentration of algae was monitored by hemocytometer measurement at 24, 48, and 72 h.

Toxicity Test toward D. magna. Five young daphnids (aged less than 24 h) were exposed to each 40 mL test solution of different concentrations of target compounds (stock solutions were prepared in acetone) or control solutions (water test control and solvent test control) in test vessels. Each treatment contained four replicates. The daphnids were incubated at a temperature of 20 ± 1 °C with the photoperiod of 16 h/8 h (light/dark) and were not fed during the experiment. The mortality of daphnids were recorded at an exposure time of 24 and 48 h.

Toxicity Test toward D. rerio. Ten fish were exposed to the test solutions (3 L) of different concentrations of *rac*-imazalil and its enantiomers. A static test was adopted because the concentrations of the test solution were satisfactorily maintained and were no less than 80% of the initial concentrations during the experiment. The treatment groups and control groups (blank control group and solvent control group) contained three repeats for each group with acetone content lower than 0.1 mL/L. Mortalities were recorded every 24 h after treatment until 96 h.

Field Experiment. The field trial was conducted according to the Guidelines for Pesticide Residue Field Trials (NY/T 788−2004) in a greenhouse at Langfang, Hebei province, where imazalil has never been applied before. The physiochemical properties of Hebei soil were as follows: soil type (brown loam); pH (7.8); organic matter (12.0 g/kg); and soil texture (15.1% sand, 45.1% silt, 39.8% clay). The tomato and cucumber seeds were purchased from Botong Nongyi Seeds (Beijing, China). The dissipation experiments of imazalil in tomato and cucumber were performed on a 30 m^2 trial plot, and each treatment contained three repeated plots. The *rac*-imazalil commercial products (15% fumigant) were applied at 0.45 g/m^2 (1.5 times the recommended dose). The representative samples (approximately 1000 g of tomato, cucumber, and soil (0−10 cm); 100 g of tomato leaves and cucumber leaves) were gathered at 4 h and 1, 3, 5, 7, 14, 21, 28, and 35 d after application, and the blank samples were collected before treatment. All the samples were homogenized and were stored at −20 °C.

Data Analysis. The thermodynamic parameters were calculated from the Van't Hoff equations:[22]

$$\ln k = -\Delta H^\circ/RT + \Delta S^\circ/R + \ln \phi \quad (1)$$

$$\ln \alpha = -\Delta\Delta H^\circ/RT + \Delta\Delta S^\circ/R \quad (2)$$

where R is the ideal gas constant, T presents the absolute temperature, and ϕ is the phase ratio. ΔH° and $\Delta\Delta H^\circ$ are the standard enthalpy

DOI: 10.1021/acs.jafc.9b03848
J. Agric. Food Chem. 2019, 67, 11331−11339

change and $(\Delta H^{\circ}_2 - \Delta H^{\circ}_1)$ separately. ΔS° and $\Delta\Delta S^{\circ}$ represent the standard entropy change and $(\Delta S^{\circ}_2 - \Delta S^{\circ}_1)$, respectively.

The percent inhibition for fungicidal activity was calculated according to the equation:[23]

$$\text{inhibition (\%)} = \frac{\text{colony diameter of control} - \text{colony diameter of treatment}}{\text{colony diameter of control} - 5\text{ cm}} \times 100 \quad (3)$$

The algae growth inhibition rate was calculated in accordance with the equation:

$$\text{inhibition (\%)} = \frac{\text{biomass concentration of (control} - \text{treatment)}}{\text{biomass concentration of control}} \times 100 \quad (4)$$

The EC_{50} representing the median effective concentration of pesticide was obtained by probit analysis by SPSS Statistics version 17.0 software. The LC_{50} (the test compounds caused 50% mortality) was calculated based on the survival data using probit analysis by SPSS Statistics software.

The enantiomeric fraction (EF) was used to assess enantioselective dissipation of enantiomers of imazalil and imazalil-M in field samples, and the calculation formula was as follows:[24]

$$\text{EF} = \frac{(+)\text{-enantiomer}}{(+)\text{-enantiomer} + (-)\text{-enantiomer}} \quad (5)$$

The dissipation kinetics of enantiomers of imazalil and imazalil-M in field samples were evaluated according to the first-order kinetics with the following equations:[22]

$$C = C_0 e^{-kt} \quad (6)$$

$$T_{1/2} = \ln 2/k \quad (7)$$

where C_0 and C were the concentrations of relevant enantiomers at the initial time ($t = 0$) and time t, respectively, and k represents degradation rate constant. SAS (version 9.4, SAS Institute, Beijing, China) was used for data analysis, and the significance difference is shown for P value < 0.05.

RESULTS AND DISCUSSION

Optimization of Chromatographic Separation. Chromatographic parameters, including chiral stationary phases (CSPs), mobile phase composition, additive, flow rate, and column temperature, could affect chiral separation of enantiomers.[25] Two amylose-based columns (Chiralpak AD-RH, Chiralpak IH) and four cellulose-based columns (Lux Cellulose-2, Chiralpak OJ-RH, Chiralpak IC-3, Chiralpak OD-RH, Table S2) were evaluated for chiral separation of four enantiomers of imazalil and imazalil-M. A commonly used mobile phase (ACN/10 mM ammonium formate in ultrapure water) was used for systemic screening of a suitable column within the allowable pressure. Simultaneous baseline separation of enantiomers of imazalil and imazalil-M was achieved on Chiralpak IH (Figure 2). The four enantiomers could be partly or could not be separated by the other columns. Thus, the Chiralpak IH column was used for further condition optimization.

The mobile phase is an important influencing factor in chiral recognition by affecting the chiral interaction environment.[26] The four enantiomers could not be separated when using ACN/water as the mobile phase, which indicated that the additive (ammonium formate) was crucial for enantioseparation of the four enantiomers. As shown in Table S3, five different mobile phase compositions (ACN/10 mM ammonium formate in ultrapure water (v/v)) were tested, and the Rs and k' decreased when the proportion of ACN increased from 45% to 65%. The 55% ACN in the mobile phase was chosen to obtain satisfying Rs and shorter RT. The Rs and k' reduced when the flow rate increased from 0.3 to 0.5 mL/min. The flow rate of 0.5 mL/min was selected with relatively short RT and acceptable Rs. Finally, column temperature was optimized from 20 to 40 °C with an interval of 5 °C. The Rs and k' gradually decreased with increasing column temperature. As shown in Table S4, thermodynamic parameters were obtained from Van't Hoff equations, and $\Delta\Delta H^{\circ}$ and $\Delta\Delta S^{\circ}$ were negative for both imazalil enantiomers and imazalil-M enantiomers, which indicated that the process of enantioseparation of imazalil and imazalil-M enantiomers was enthalpy driven.[27] Thus, the column temperature was set as 20 °C to acquire higher Rs. Finally, the chiral separation of imazalil and imazalil-M enantiomers were conducted on the Chiralpak IH column using the mobile phase of ACN/10 mM ammonium formate in ultrapure water (55:45, v/v). The flow rate and column temperature were 0.5 mL/min and 20 °C, respectively.

Confirmation of Absolute Configuration and Optical Rotation. Optical rotation and absolute configuration are an important basis for exploring the mechanism of enantioselectivity. The optical rotations were confirmed based on UPLC coupled with an advanced laser polarimeter detector. The elution order was (+)-imazalil, (−)-imazalil, (+)-imazalil-M, and (−)-imazalil-M, successively. The absolute configurations of imazalil and imazalil-M enantiomers were confirmed by comparing the theoretically calculated electronic circular dichroism (ECD) spectrum with experimental ECD (Figure 2). The calculated ECD spectra for *S*-enantiomer and *R*-enantiomer basically coincided with experimental ECD spectra of peak 1 and peak 2, respectively. Thus, the elution orders of the four enantiomers were confirmed as *S*-(+)-imazalil, *R*-(−)-imazalil, *S*-(+)-imazalil-M, and *R*-(−)-imazalil-M, successively. The absolute configurations of imazalil enantiomers were also reported by a patent, formerly, where *S*-imazalil was the dextro-isomer and *R*-imazalil was the levo-enantiomer.[13] The results were in agreement with the conclusion in the patent.

Stability of the Enantiomers. The relative standard deviations (RSDs) were all below 20% by comparing the initial concentrations with tested concentrations of four enantiomers of imazalil and imazalil-M in ACN, acetone, and water at different sampling times during the experiment. The isomerization of enantiomers was also not found in these solvents during the experiment. Furthermore, the photostability of the two enantiomers of imazalil was explored. The two enantiomers of imazalil exhibited a similar dissipation rate in nine kinds of test solvents. The configurations of the two enantiomers were stable, and no enantiomerization was found during the photolysis experiment. The half-lives of imazalil enantiomers were 7.5−45.6 h, and the dissipation order was as follows: IPA > ethyl acetate > MeOH > acetone ≈ aqueous buffers (pH 4) > ACN > aqueous buffers (pH 9) > aqueous buffers (pH 7) > ultrapure water (Table S5).

Biotest with *Rac*-Imazalil and Pure Enantiomers. Seven typical pathogens were selected which caused tomato leaf mold, tomato early blight, tomato late blight, tomato gray mold, grape or apple bitter rot, apple canker, and green mold of citrus. The biological activities of *rac*-imazalil and its enantiomers toward seven pathogens were different, and EC_{50} values are shown in Table 1. The order of bioactivities

DOI: 10.1021/acs.jafc.9b03848
J. Agric. Food Chem. 2019, 67, 11331−11339

Table 1. Fungicidal Activities of *rac*-Imazalil and Its Two Enantiomers Aganist Seven Plant Pathogens

	rac-imazalil		*S*-(+)-imazalil		*R*-(−)-imazalil	
pathogen	EC_{50} (mg/L)	R^{2b}	EC_{50} (mg/L)	R^2	EC_{50} (mg/L)	R^2
Fulvia fulva	0.145 (0.111−0.186)[a]	0.986	0.099 (0.073−0.132)	0.983	0.544 (0.431−0.683)	0.982
Alternaria solani	0.201 (0.160−0.251)	0.994	0.109 (0.083−0.141)	0.983	0.718 (0.573−0.902)	0.987
Phytophthora infestans	1.244 (0.861−1.937)	0.976	0.915 (0.626−1.428)	0.970	2.749 (1.914−4.276)	0.967
Botrytis cinerea	4.494 (3.743−5.552)	0.971	3.252 (2.489−4.599)	0.997	14.423 (10.397−21.913)	0.964
Glomerella cingulata	2.466 (1.964−3.084)	0.990	1.131 (0.893−1.446)	0.997	6.654 (4.945−9.218)	0.994
Valsa mali	7.773 (6.244−9.809)	0.978	4.676 (3.685−6.045)	0.977	30.806 (24.987−41.209)	0.989
Penicillium digitatum	3.356 (2.465−4.669)	0.965	2.439 (1.820−3.150)	0.990	11.466 (8.269−17.440)	0.961

[a]The value represents 95% confidence intervals. [b]R^2 represents correlation coefficients.

exhibited consistency and was *S*-(+)-imazalil > *rac*-imazalil > *R*-(−)-imazalil. *S*-(+)-imazalil showed 3.00−6.59 times higher fungicidal activity than *R*-(−)-imazalil toward different pathogens in in vitro study. The results were in agreement with a previous study, where the *S*-(+)-imazalil was 1.02−5.06 times more effective toward *Phytophthora infestans* (tested on tomato), *Pyricularia oryzae* (rice), *Botrytis cineria* (pepper), *Erysiphe graminis* (wheat), and *Puccinia recondita* (wheat) for inoculated plants than *R*-isomer under the filed conditions.[11] *S*-(+)-Imazalil also showed 10 times higher bioactivity toward *Aspergillus nidulans* than *R*-(−)-imazalil in in vitro study according to the literature.[11] Considering that the configurations of imazalil enantiomers were stable, the development of *S*-(+)-imazalil may be more potent for controlling various fungal diseases. Usually, one enantiomer of chiral fungicide has a stronger fungicidal activity than the others. For instance, *R*-flutriafol showed 1.49−6.23 times higher bioactivity than *S*-flutriafol toward five target pathogens.[28] (−)-Hexaconazole was 1.26−13.45 times more active than (+)-hexaconazole against four target pathogens.[29] The bioactivity of (*2R,4S*)-difenoconazole was more than the other three stereoisomers with the order (*2R,4S*) > (*2R,4R*) > (*2S,4R*) > (*2S,4S*) for four pathogens.[6] However, the orders of fungicidal activity of four stereoisomers of propiconazole were dependent on pathogenic species.[30] The enantioselectivity of bioactivity of chiral fungicide may be derived by binding to chiral biomolecules and biological receptors which are structure sensitive.[28] The difference in binding affinity between the two enantiomers of imazalil and binding sites of the receptor was explored by a molecular docking study as discussed in the next section.

Molecular Docking. Previous studies showed that azole fungicides are heme coordinating inhibitors of sterol 14α-demethylase (CYP51) generally, and bonding modes between azole fungicides and amino acid residues are mainly nonbond interactions including hydrophobic interaction, van der Waals interaction, hydrogen bonds, aromatic stacking interactions, etc.[31,32] The protein sequences of CYP51 of seven typical pathogens were searched in the UniProt database (https://www.uniprot.org/). Only two protein sequences, including *P. digitatum* CYP51 (Uniprot code: Q8TFI9) and *B. cinerea* CYP51 (Uniprot code: Q9P428), could be found. Thus, the two represented *P. digitatum* CYP51 and *B. cinereal* for further study. The crystal structure of CYP51B of *Aspergillus fumigatus* was used as a template which shared a high sequence identity (66.24%) with *P. digitatum* CYP51. The interaction between imazalil and CYP51 of *P. digitatum* was explored by molecular docking. As shown in Figure 3, the active site of CYP51 of *P. digitatum* formed a hydrophobic cavity. The imidazolyl of *S*-(+)-imazalil and *R*-(−)-imazalil formed a coordination bond with heme. 2,4-Dichlorophenyl of *S*-(+)-imazalil and *R*-(−)-imazalil had a hydrophobic interaction with Tyr126, Phe120, Thr301, and Ala305. However, the bond conformations of allyloxy were different between *S*-(+)-imazalil and *R*-(−)-imazalil. For *R*-enantiomer, the double bond of allyloxy paralleled to Tyrl12 and had a hydrophobic interaction with Tyrl12 and Tyr126. For *S*-enantiomer, the double bond of allyloxy had a hydrophobic interaction with Ile371 and Tyrl12. The conformation not only enhanced the hydrophobic interaction but also made energy conformation by the combination of *S*-enantiomer and binding site of receptor protein lower than that for *R*-enantiomer. Furthermore, the better grid score for *S*-(+)-imazalil (−41.17 kcal/mol) than *R*-(−)-imazalil (−39.93 kcal/mol) indicated that *S*-(+)-imazalil has a better binding ability to CYP51 of *P. digitatum* than *R*-(−)-imazalil. The molecular docking results were consistent with enantioselective bioactivity study and could partly explain its inherent mechanism.

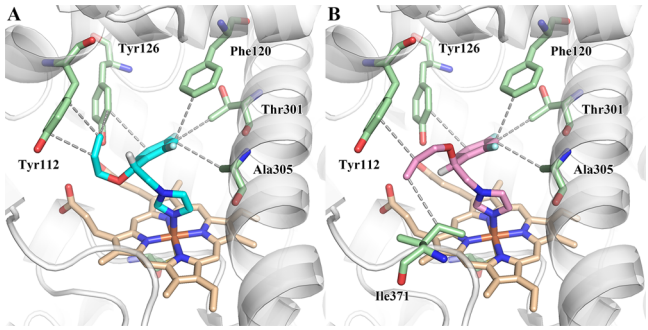

Figure 3. Model of combination mode between CYP51 and *R*-(−)-imazalil (A) or *S*-(+)-imazalil (B). The secondary structure of the protein was shown as a gray cartoon and key residues were shown as pale green sticks. The heme group was shown in wheat stick form. The gray dashed line represented hydrophobic interaction. The cyan and pick sticks represent *R*-(−)-imazalil and *S*-(+)-imazalil, respectively.

Sequence alignment analysis showed high sequence similarity between the protein sequence of *P. digitatum* CYP51 and *B. cinerea* CYP51 (Figure S1 of the Supporting Information). Analysis of binding modes demonstrated that Thr301 of *P. digitatum* CYP51 had hydrophobic interaction with imazalil, and Ala304 of *B. cinereal* had a similar effect. The other contributing residues which have interactions with imazalil enantiomers in the binding pocket were all conserved amino acids. These indicated that the analysis results of molecular docking of the interaction between *P. digitatum* CYP51 and imazalil enantiomers were representative among the above two targeted pathogens.

DOI: 10.1021/acs.jafc.9b03848
J. Agric. Food Chem. 2019, 67, 11331−11339

Table 2. Aquatic Toxicity of Racemate and Enantiomers of Imazalil

	P. subcapitata (72 h)		*D. magna* (48 h)		*D. rerio* (96 h)	
compound	EC_{50} (mg/L)	R^{2b}	LC_{50} (mg/L)	R^2	LC_{50} (mg/L)	R^2
rac-imazalil	0.623 (0.476−0.782)[a]	0.939	0.882 (0.753−1.051)	0.982	2.324 (2.192−2.418)	0.928
S-(+)-imazalil	0.664 (0.559−0.779)	0.972	0.665 (0.538−0.783)	0.954	3.094 (2.969−3.312)	0.877
R-(−)-imazalil	0.818 (0.619−1.067)	0.950	1.493 (1.170−2.055)	0.990	2.548 (2.454−2.648)	0.991

[a]The value represents 95% confidence intervals. [b]R^2 represents correlation coefficients.

Table 3. Aquatic Toxicity of Racemate and Enantiomers of Imazalil-M

	P. subcapitata (72 h)		*D. magna* (48 h)	
compound	EC_{50} (mg/L)	R^{2b}	LC_{50} (mg/L)	R^2
rac-imazalil-M	2.611 (2.261−3.017)[a]	0.977	11.251 (9.041−13.872)	0.979
S-(+)-imazalil-M	1.552 (1.439−1.673)	0.977	8.461 (5.724−11.016)	0.978
R-(−)-imazalil-M	3.429 (2.581−4.551)	0.936	14.388 (12.781−15.990)	0.953

[a]The value represents 95% confidence intervals. [b]R^2 represents correlation coefficients.

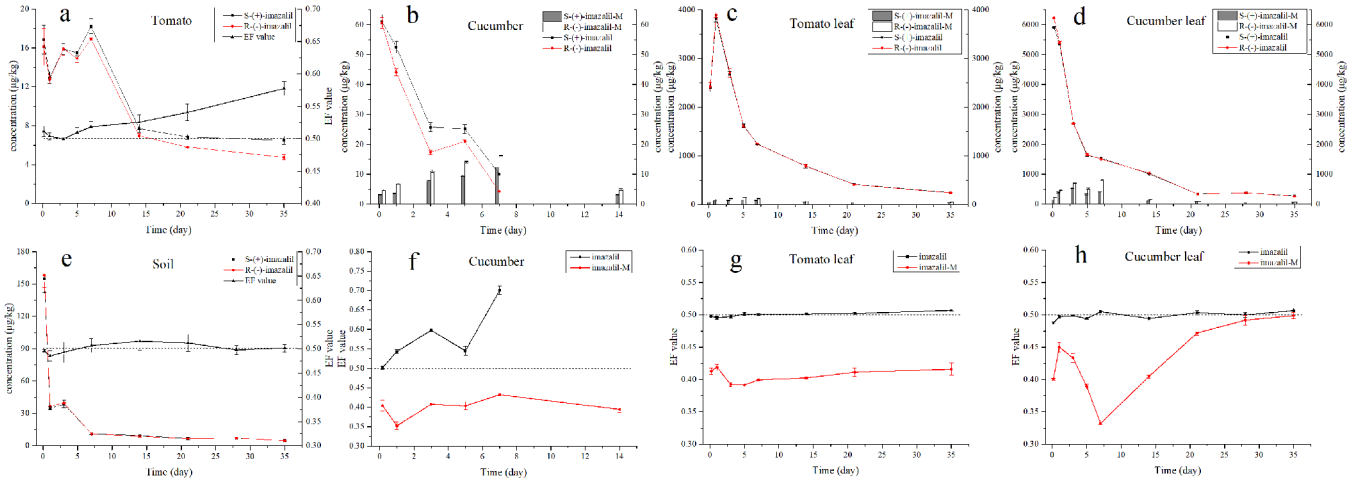

Figure 4. Enantiomers concentration and EF values of imazalil and imazalil-M during degradation in tomato (a), cucumber (b, f), tomato leaf (c, g), cucumber leaf (d, h), and soil (e).

Table 4. Dissipation Equations of Imazalil Enantiomers in Tomato, Cucumber, Tomato Leaf, Cucumber Leaf and soil

matrix	enantiomer	degradation equation	R^2	$T_{1/2}$ (days)[a]	P^b
tomato	*S*-(+)-imazalil	$C_t = 16.26e^{-0.0311t}$	0.7438	22.29 ± 1.14	0.0101[c]
	R-(−)-imazalil	$C_t = 16.20e^{-0.0394t}$	0.8341	17.59 ± 0.34	
cucumber	*S*-(+)-imazalil	$C_t = 64.66e^{-0.2468t}$	0.9332	2.81 ± 0.05	0.0019[c]
	R-(−)-imazalil	$C_t = 63.66e^{-0.3416t}$	0.8743	2.03 ± 0.02	
tomato leaf	*S*-(+)-imazalil	$C_t = 2584.42e^{-0.0778t}$	0.9203	8.91 ± 0.07	0.0023[c]
	R-(−)-imazalil	$C_t = 2608.10e^{-0.0789t}$	0.9204	8.79 ± 0.08	
cucumber leaf	*S*-(+)-imazalil	$C_t = 3732.13e^{-0.0862t}$	0.8875	8.04 ± 0.04	0.0160[c]
	R-(−)-imazalil	$C_t = 3812.33e^{-0.0875t}$	0.8866	7.92 ± 0.03	
soil	*S*-(+)-imazalil	$C_t = 45.69e^{-0.0753t}$	0.7042	9.24 ± 0.25	0.4361
	R-(−)-imazalil	$C_t = 46.33e^{-0.0766t}$	0.6982	9.11 ± 0.22	

[a]Values refer to the means ± STDEVs (n = 3). [b]P values from dissipation half-lives ($T_{1/2}$) between *S*-(+)-imazalil and *R*-(−)-imazalil using Student's paired t test at 95% probability. [c]Values represent a statistically significant difference ($P < 0.05$).

Enantioselectivity in Acute Aquatic Toxicity. The acute aquatic toxicities of racemates and enantiomers of imazalil and imazalil-M toward aquatic organisms were evaluated, which were expressed by EC_{50} and LC_{50}. The acute toxicity data for imazalil and imazalil-M are summarized in Tables 2 and 3, respectively. The varied toxicity between *rac*-imazalil and its two enantiomers toward *P. subcapitata*, *D. magna*, and *D. rerio* were observed. The order of acute toxicity toward *D. magna* and *P. subcapitata* was *S*-(+)-imazalil > *rac*-imazalil > *R*-(−)-imazalil, and *S*-(+)-imazalil showed 1.23−2.25 times higher toxicity than *R*-(−)-imazalil. However, the order of acute toxicity to *D. rerio* was *rac*-imazalil > *R*-(−)-imazalil > *S*-(+)-imazalil, and the acute toxicity of *R*-(−)-imazalil was 1.21 times higher than *S*-(+)-imazalil. The major metabolite imazalil-M also showed enantioselectivity in aquatic toxicity. *S*-(+)-Imazalil-M exhibited 2.21 times and 1.70 times greater acute toxicity than *R*-(−)-imazalil-M to *P. subcapitata* and *D. magna*, respectively. The order of toxic

DOI: 10.1021/acs.jafc.9b03848
J. Agric. Food Chem. 2019, 67, 11331−11339

potency was *S*-(+)-imazalil-M > *rac*-imazalil-M > *R*-(−)-imazalil-M. The extent and trend of enantioselectivity of toxicity toward nontarget organisms between the enantiomers usually differs depending on the species of nontarget organisms.[30,33−35] Although the acute toxicity of imazalil-M was lower than for imazalil, its toxicity should not be ignored and should be monitored in the environment. Therefore, the toxicity assessment of imazalil was unreasonable only based on *rac*-imazalil. Many studies have focused on analyzing the molecular mechanisms of enantioselective toxicity, for example, difference in genomic expression, stress protein response, etc.[36,37] Thus, the mechanism of enantioselectivity in toxicity of imazalil and imazalil-M enantiomers could be explored in further studies. The results of these studies could provide information for accurate risk assessment of imazalil and offer toxicological data for recommending single-enantiomer products of imazalil.

Stereoselective Dissipation of Imazalil under Greenhouse Conditions. Generally, the concentration of imazalil enantiomers decreased gradually with time prolonged in all matrices after application of the fumigant of imazalil (Figure 4). The residues reached their highest amount at 1 d in tomato leaf and fluctuated in tomato for the first 7 days, followed by a gradually decrease. The initially increasing trend may result from redeposition of imazalil. The difference in original accumulation in different plants may be caused by fruit or leaf shape, structure of the surface layer, etc. The dissipation of imazalil enantiomers basically followed first-order kinetics with R^2 ranging from 0.6982 to 0.9332 (Table 4). The half-lives of *S*-(+)-imazalil and *R*-(−)-imazalil were between 2.03 ± 0.02 days and 22.29 ± 1.14 days in all matrices (Table 4). The $T_{1/2}$ of *S*-(+)-imazalil and *R*-(−)-imazalil were significantly different ($P < 0.05$, Student's paired *t*-test) in all matrices except in soil, which indicated that enantioselective dissipation occurred in tomato, cucumber, tomato leaf, and cucumber leaf. Furthermore, the degradation rates of imazalil in cucumber and cucumber leaf were faster than that in tomato and tomato leaf, respectively ($P < 0.05$, Student's paired *t*-test). The difference may be due to the difference in the degrading enzyme system of plants.

The EF values were also calculated to assess enantioselectivity. The EF values increased from 0.511 ± 0.008 (4 h) to 0.578 ± 0.008 (35 d) in tomato, from 0.502 ± 0.004 (4 h) to 0.700 ± 0.011 (7 d) in cucumber, and from 0.498 ± 0.001 (4 h) to 0.507 (35 d) in tomato leaf, and from 0.487 ± 0.002 (4 h) to 0.507 ± 0.004 (35 d) in cucumber leaf. The difference of EF values between the 2 days were significant ($P < 0.05$, Student's paired *t*-test). The EF values fluctuated around 0.5 in soil, and no significant difference ($P > 0.05$) was observed between 0.495 ± 0.004 (4 h) and 0.501 ± 0.008 (35 d). Thus, no significant enantioselective degradation of imazalil occurred in soil under greenhouse conditions in Hebei province. The result of nonenantioselectivity in soil was consistent with previous study under five treatment conditions in laboratory and in three kinds of soil from three sites.[19,38] *R*-(−)-Imazalil was more preferentially degraded than *S*-(+)-imazalil in tomato and cucumber, resulting in enrichment of *S*-(+)-imazalil, and *R*-(−)-imazalil degraded slightly faster than high-effective *S*-(+)-imazalil in tomato leaf and cucumber leaf, which was beneficial to disease control. Enantioselective trends of imazalil were reported to be different between different species, varieties, and parts of the plant.[12,19−21] Stereoselective translocation and dissipation of imazalil was reported to exist in plants simultaneously.[12] A functional enzymatic system was generally considered as the important factor for enantioselective behavior in the biological system.[39] In this study, the intensity of enantioselective trend in fruit was much higher than in leaves, which may result from a different enzyme activity in different parts of plants. The mechanism of enantioselective dissipation should be explored in future studies.

The Formation of Imazalil-M under Greenhouse Conditions. The metabolite imazalil-M was detected, and approximately 27.3%, 3.6% and 11.8% of imazalil was transformed to imazalil-M in cucumber, tomato leaf, and cucumber leaf, respectively (Figure 4). In cucumber, the concentration of *S*-(+)-imazalil-M and *R*-(−)-imazalil-M gradually increased to a maximum of 12.4 and 16.3 μg/kg at 7 days, respectively, and then the residue of the enantiomers decreased. The EF of imazalil-M was initially decreased and then increased generally. For tomato leaf and cucumber leaf, the concentrations of imazalil-M enantiomers reached a maximum at 5 days (93.8 μg/kg for *S*-(+)-imazalil-M and 145.7 μg/kg for *R*-(−)-imazalil-M) and 3 days (539.4 μg/kg for *S*-(+)-imazalil-M and 703.9 μg/kg for *R*-(−)-imazalil-M), separately. In tomato leaf, the EF of imazalil-M was increased from 0.413 (4 h) to 0.419 (1 d), then decreased to 0.392 (3 d), and slightly increased to 0.416 (35 d) afterward. In cucumber leaf, the EF of imazalil-M was increased from 0.401 (4 h) to 0.450 (1 d) and then decreased obviously to 0.332 (7 d), followed by an increasing trend from 0.332 (7 d) to 0.499 (35 d). The phenomenon was caused by the comprehensive effect of enantioselective metabolism of imazalil enantiomers and enantioselective degradation of imazalil-M enantiomers. Considering the unneglectable toxicity of imazalil-M, it is important to monitor imazalil-M enantiomers in food and the environment.

This is the first report for a comprehensive evaluation of enantiomers of imazalil and imazalil-M considering enantioselective bioactivity, aquatic toxicity, and environmental fate. The results indicated that the more highly effective *S*-(+)-imazalil also had more toxicity to *D. magna* and *P. subcapitata*. However, the acute toxicity of the higher effective *S*-(+)-imazalil was little lower than that of *R*-(−)-imazalil to *D. rerio*. Furthermore, the toxicity of imazalil-M should not be overlooked. *S*-(+)-Imazalil-M showed a higher toxicity than *R*-(−)-imazalil-M to *P. subcapitata* and *D. magna*. By comprehensive consideration, development of *S*-(+)-imazalil was recommended for decreasing the chemical consumption and reducing the risk to *D. rerio*. The enantioselective dissipation trend of imazalil in edible parts was more significant than in leaves of cucumber and tomato, and high-effective *S*-(+)-imazalil was preferentially enriched. Furthermore, imazalil-M enantiomers easily formed in tomato and cucumber leaves and cucumber fruit. Thus, the risk of imazalil was underestimated according to traditional risk assessment. The results emphasized the importance for monitoring the metabolite of pesticide and distinguishing the difference between the enantiomers for accurate risk assessment.

■ ASSOCIATED CONTENT

Supporting Information

The Supporting Information is available free of charge on the ACS Publications website at DOI: 10.1021/acs.jafc.9b03848.

DOI: 10.1021/acs.jafc.9b03848
J. Agric. Food Chem. 2019, 67, 11331−11339

Study on photostability of imazalil enantiomers, the instrumental conditions for enantioseparation of imazalil and imazalil-M based on UPLC-MS/MS, confirmation of optical rotation and absolute configuration, method for molecular docking, details of sequence alignment analysis of CYP51 of *Penicillium digitatum* and *Botrytis cinereal*, sample pretreatment methods and optimization, and method validation for residue analysis (PDF)

AUTHOR INFORMATION

Corresponding Author

*E-mail: dongfengshou@caas.cn. Tel.: +86 10 62815938. Fax: +86 10 62815938.

ORCID

Fengshou Dong: 0000-0001-5375-3397

Yongquan Zheng: 0000-0002-1676-035X

Funding

This work was financially supported by the National Natural Science Foundation of China (31872004).

Notes

The authors declare no competing financial interest.

REFERENCES

(1) Verger, P. J. P.; Boobis, A. R. Reevaluate pesticides for food security and safety. *Science* **2013**, *341*, 717−718.

(2) Ying, Z.; Ling, L.; Kunde, L.; Xinping, Z.; Weiping, L. Enantiomer separation of triazole fungicides by high-performance liquid chromatography. *Chirality* **2009**, *21*, 421−427.

(3) Ye, J.; Zhao, M.; Niu, L.; Liu, W. Enantioselective environmental toxicology of chiral pesticides. *Chem. Res. Toxicol.* **2015**, *28*, 325−338.

(4) Ye, J.; Zhao, M.; Liu, J.; Liu, W. Enantioselectivity in environmental risk assessment of modern chiral pesticides. *Environ. Pollut.* **2010**, *158*, 2371−2383.

(5) Zhan, X.; Liu, H.; Miao, Y.; Liu, W. A comparative study of *rac*- and *S*-metolachlor on some activities and metabolism of silkworm, *Bombyx mori* L. *Pestic. Biochem. Physiol.* **2006**, *85*, 133−138.

(6) Dong, F.; Li, J.; Chankvetadze, B.; Cheng, Y.; Xu, J.; Liu, X.; Li, Y.; Chen, X.; Bertucci, C.; Tedesco, D.; Zanasi, R.; Zheng, Y. Chiral triazole fungicide difenoconazole: absolute stereochemistry, stereoselective bioactivity, aquatic toxicity, and environmental behavior in vegetables and soil. *Environ. Sci. Technol.* **2013**, *47*, 3386−3394.

(7) Kenneke, J. F.; Mazur, C. S.; Kellock, K. A.; Overmyer, J. P. Mechanistic approach to understanding the toxicity of the azole fungicide triadimefon to a nontarget aquatic insect and implications for exposure assessment. *Environ. Sci. Technol.* **2009**, *43*, 5507−5513.

(8) Faniband, M. H.; Littorin, M.; Ekman, E.; Jönsson, B. A. G.; Lindh, C. H. LC−MS-MS analysis of urinary biomarkers of imazalil following experimental exposures. *J. Anal. Toxicol.* **2015**, *39*, 691−697.

(9) Matsumoto, H. Simultaneous Determination of imazalil and its major metabolite in citrus fruit by solid-phase extraction and capillary gas chromatography with electron capture detection. *J. AOAC Int.* **2001**, *84* (2), 546−550.

(10) Yoshioka, N.; Akiyama, Y.; Teranishi, K. Rapid simultaneous determination of o-phenylphenol, diphenyl, thiabendazole, imazalil and its major metabolite in citrus fruits by liquid chromatography-mass spectrometry using atmospheric pressure photoionization. *J. Chromatogr. A* **2004**, *1022*, 145−150.

(11) Vass, A.; Korpics, E.; Dernovics, M. Follow-up of the fate of imazalil from post-harvest lemon surface treatment to a baking experiment. *Food Addit. Contam., Part A* **2015**, *32*, 1875−1884.

(12) Lv, T.; Carvalho, P. N.; Casas, M. E.; Bollmann, U. E.; Arias, C. A.; Brix, H.; Bester, K. Enantioselective uptake, translocation and degradation of the chiral pesticides tebuconazole and imazalil by Phragmites australis. *Environ. Pollut.* **2017**, *229*, 362−370.

(13) Nelson, R. A.; Thomas, N. W.; Matcham, G. W.; Lin, S. L.; Zhang, M.; Lewis, C. M., Chiral imidazole fungicidal compositions and methods for their use. U.S. Patent 6,207,695 B1, 2001.

(14) Lv, T.; Zhang, Y.; Casas, M. E.; Carvalho, P. N.; Arias, C. A.; Bester, K.; Brix, H. Phytoremediation of imazalil and tebuconazole by four emergent wetland plant species in hydroponic medium. *Chemosphere* **2016**, *148*, 459−466.

(15) Belenguer, V.; Martinez-Capel, F.; Masiá, A.; Picó, Y. Patterns of presence and concentration of pesticides in fish and waters of the Júcar River (Eastern Spain). *J. Hazard. Mater.* **2014**, *265*, 271−279.

(16) Ccanccapa, A.; Masiá, A.; Andreu, V.; Picó, Y. Spatio-temporal patterns of pesticide residues in the Turia and Júcar Rivers (Spain). *Sci. Total Environ.* **2016**, *540*, 200−210.

(17) Castillo, L. E.; Martínez, E.; Ruepert, C.; Savage, C.; Gilek, M.; Pinnock, M.; Solis, E. Water quality and macroinvertebrate community response following pesticide applications in a banana plantation, Limon, Costa Rica. *Sci. Total Environ.* **2006**, *367*, 418−432.

(18) Jin, Y.; Zhu, Z.; Wang, Y.; Yang, E.; Feng, X.; Fu, Z. The fungicide imazalil induces developmental abnormalities and alters locomotor activity during early developmental stages in zebrafish. *Chemosphere* **2016**, *153*, 455−461.

(19) Li, R.; Dong, F.; Xu, J.; Liu, X.; Wu, X.; Pan, X.; Tao, Y.; Chen, Z.; Zheng, Y. Enantioseparation of imazalil and monitoring its enantioselective degradation in apples and soil using ultra-high performance liquid chromatography/tandem mass spectrometry. *J. Agric. Food Chem.* **2017**, *65*, 3259−3267.

(20) Ruiz-Rodríguez, L.; Aguilar, A.; Díaz, A. N.; Sánchez, F. G. Enantioseparation of the fungicide imazalil in orange juice by chiral HPLC. Study on degradation rates and extractive/enrichment techniques. *Food Chem.* **2015**, *178*, 179−185.

(21) Kodama, S.; Yamamoto, A.; Ohura, T.; Matsunaga, A.; Kanbe, T. Enantioseparation of imazalil residue in orange by capillary electrophoresis with 2-hydroxypropyl-beta-cyclodextrin as a chiral selector. *J. Agric. Food Chem.* **2003**, *51*, 6128−6131.

(22) Chen, Z.; Dong, F.; Xu, J.; Liu, X.; Cheng, Y.; Liu, N.; Tao, Y.; Pan, X.; Zheng, Y. Stereoselective separation and pharmacokinetic dissipation of the chiral neonicotinoid sulfoxaflor in soil by ultraperformance convergence chromatography/tandem mass spectrometry. *Anal. Bioanal. Chem.* **2014**, *406*, 6677−6690.

(23) Zhang, Q.; Zhang, Z.; Tang, B.; Gao, B.; Tian, M.; Sanganyado, E.; Shi, H. Y.; Wang, M. Mechanistic insights into stereospecific bioactivity and dissipation of chiral fungicide triticonazole in agricultural management. *J. Agric. Food Chem.* **2018**, *66*, 7286−7293.

(24) Pan, X.; Dong, F.; Xu, J.; Liu, X.; Chen, Z.; Zheng, Y. Stereoselective analysis of novel chiral fungicide pyrisoxazole in cucumber, tomato and soil under different application methods with supercritical fluid chromatography/tandem mass spectrometry. *J. Hazard. Mater.* **2016**, *311*, 115−124.

(25) Lämmerhofer, M. Chiral recognition by enantioselective liquid chromatography: Mechanisms and modern chiral stationary phases. *J. Chromatogr. A* **2010**, *1217*, 814−856.

(26) Yao, Z.; Li, X.; Miao, Y.; Lin, M.; Xu, M.; Wang, Q.; Zhang, H. Simultaneous enantioselective determination of triadimefon and its metabolite triadimenol in edible vegetable oil by gel permeation chromatography and ultraperformance convergence chromatography/tandem mass spectrometry. *Anal. Bioanal. Chem.* **2015**, *407*, 8849−8859.

(27) Zhang, Z.; Zhang, Q.; Gao, B.; Gou, G.; Li, L.; Shi, H. Y.; Wang, M. H. Simultaneous enantioselective determination of the chiral fungicide prothioconazole and its major chiral metabolite prothioconazole-desthio in food and environmental samples by ultra-performance liquid chromatography tandem mass spectrometry. *J. Agric. Food Chem.* **2017**, *65*, 8241−8247.

(28) Zhang, Q.; Shi, H.; Liu, J.; Tian, M.; Wang, M.; Hua, X.-D. Enantioselective bioactivity, acute toxicity and dissipation in vegetables of the chiral triazole fungicide flutriafol. *J. Hazard. Mater.* **2015**, *284*, 65−72.

DOI: 10.1021/acs.jafc.9b03848
J. Agric. Food Chem. 2019, 67, 11331−11339

(29) Han, J.; Jiang, J.; Su, H.; Sun, M.; Wang, P.; Liu, D.; Zhou, Z. Bioactivity, toxicity and dissipation of hexaconazole enantiomers. *Chemosphere* **2013**, *93*, 2523−2527.
(30) Pan, X.; Cheng, Y.; Dong, F.; Liu, N.; Xu, J.; Liu, X.; Wu, X.; Zheng, Y. Stereoselective bioactivity, acute toxicity and dissipation in typical paddy soils of the chiral fungicide propiconazole. *J. Hazard. Mater.* **2018**, *359*, 194−202.
(31) Friggeri, L.; Hargrove, T. Y.; Wawrzak, Z.; Blobaum, A. L.; Rachakonda, G.; Lindsley, C. W.; Villalta, F.; Nes, W. D.; Botta, M.; Guengerich, F. P.; Lepesheva, G. I. Sterol 14α-demethylase structure-based design of VNI (((R)-N-(1-(2, 4-dichlorophenyl)-2-(1H-imidazol-1-yl) ethyl)-4-(5-phenyl-1, 3, 4-oxadiazol-2-yl) benzamide)) derivatives to target fungal infections: synthesis, biological evaluation, and crystallographic analysis. *J. Med. Chem.* **2018**, *61*, 5679−5691.
(32) Qian, H.; Duan, M.; Sun, X.; Chi, M.; Zhao, Y.; Liang, W.; Du, J.; Huang, J.; Li, B. The binding mechanism between azoles and FgCYP51B, sterol 14α-demethylase of Fusarium graminearum. *Pest Manage. Sci.* **2018**, *74*, 126−134.
(33) Li, Y.; Dong, F.; Liu, X.; Xu, J.; Han, Y.; Zheng, Y. Enantioselectivity in tebuconazole and myclobutanil non-target toxicity and degradation in soils. *Chemosphere* **2015**, *122*, 145−153.
(34) Cui, N.; Xu, H.; Yao, S.; He, Y.; Zhang, H.; Yu, Y. Chiral triazole fungicide tebuconazole: enantioselective bioaccumulation, bioactivity, acute toxicity, and dissipation in soils. *Environ. Sci. Pollut. Res.* **2018**, *25*, 25468−25475.
(35) Qi, S. Z.; Chen, X. F.; Liu, Y.; Jiang, J. Z.; Wang, C. J. Comparative toxicity of rac- and S-tebuconazole to Daphnia magna. *J. Environ. Sci. Health, Part B* **2015**, *50*, 456−462.
(36) Wang, C.; Lu, D.; Yang, J.; Xu, Y.; Gong, C.; Li, Z. Enantioselective Phytotoxicity and the Relative Mechanism of Current Chiral Herbicides. *Curr. Protein Pept. Sci.* **2016**, *18*, 15−21.
(37) Lu, X. Enantioselective effect of bifenthrin on antioxidant enzyme gene expression and stress protein response in PC12 cells. *J. Appl. Toxicol.* **2013**, *33*, 586−592.
(38) Chu, B.-L.; Guo, B.-Y.; Peng, Z.; Wang, Z.; Guo, G.; Lin, J.-M. Studies on degradation of imazalil enantiomers in soil using capillary electrophoresis. *J. Sep. Sci.* **2007**, *30*, 923−929.
(39) Bagnall, J.; Malia, L.; Lubben, A.; Kasprzyk-Hordern, B. Stereoselective biodegradation of amphetamine and methamphetamine in river microcosms. *Water Res.* **2013**, *47*, 5708−5718.

DOI: 10.1021/acs.jafc.9b03848
J. Agric. Food Chem. 2019, 67, 11331−11339